NATIONAL ADVISORY COMMITTEE FOR AERONAUTICS

WARTIME REPORT

CHARTS FOR ESTIMATION OF THE CHARACTERISTICS

OF A HELICOPTER ROTOR IN FORWARD FLIGHT

I - PROFILE DRAG-LIFT RATIO

FOR UNTWISTED RECTANGULAR BLADES

By F. J. Bailey, Jr. and F. B. Gustafson

Langley Memorial Aeronautical Laboratory
Langley Field, Va.

NACA

WASHINGTON

NATIONAL ADVISORY COMMITTEE FOR AERONAUTICS

ADVANCE CONFIDENTIAL REPORT

CHARTS FOR ESTIMATION OF THE CHARACTERISTICS

OF A HELICOPTER ROTOR IN FORWARD FLIGHT

I - PROFILE DRAG-LIFT RATIO

FOR UNTWISTED RECTANGULAR BLADES

By F. J. Bailey, Jr. and F. B. Gustafson

SUMMARY

Charts showing the rotor profile drag-lift ratio
are presented for a helicopter rotor operating in
forward flight and having hinged rectangular untwisted
blades. Charts are given for a range of power input
covering glides, level flight, and moderate rates of
climb. Each chart expresses the relation between the
lift and the profile-drag characteristics of the rotor
for various combinations of pitch angle, tip-speed
ratio, and solidity for a particular value of a parameter
representing the shaft power input.

A particular drag curve, represented by a power
series, was used in preparing the charts. This curve
is compared with experimental curves for typical air-
foils. The method by which the charts may be used in
calculating the total shaft power required for any
specific flight condition is shown by an example.

The charts indicate that, for the rotor with
rectangular untwisted blades, one effect of increasing
the shaft power input is to produce a moderate increase
in the profile drag-lift ratio. They further indicate
that, regardless of the amount of power used, the
optimum profile drag-lift ratio is obtained at the
highest pitch angles permitted by the high section
angles of attack encountered on the retreating side of
the rotor disk.

INTRODUCTION

Because of the pressing requirements of procurement agencies for a rational method for evaluation of helicopter proposals and because of the requirements of helicopter designers for a basis for choosing the optimum combination of variables, it was felt that a need existed for design charts summarizing the effect of changes in the major variables on the characteristics of a powered rotor in forward flight. The method of analysis of reference 1 accordingly was used to prepare summary charts that are generally similar to figure 3 of reference 1 but cover various amounts of shaft power input. The present report has, for simplicity, been restricted to the basic case of zero blade twist.

METHOD OF ANALYSIS

Parameter for shaft power input.- The primary modification made herein in the method of reference 1 is the introduction of a new parameter P/L for rotor-shaft power input. The symbol P represents the drag that would absorb the same power, at the velocity along the flight path, as the power being supplied through the rotor shaft. The parameter P/L is therefore equal to the total drag-lift ratio, or

$$\frac{P}{L} = \left(\frac{D}{L}\right)_o + \left(\frac{D}{L}\right)_i + \left(\frac{D}{L}\right)_p + \left(\frac{D}{L}\right)_c \qquad (1)$$

where

$\left(\frac{D}{L}\right)_o$ profile drag-lift ratio

$\left(\frac{D}{L}\right)_i$ induced drag-lift ratio

$\left(\frac{D}{L}\right)_p$ parasite drag-lift ratio

$\left(\frac{D}{L}\right)_c$ drag-lift ratio representing angle of climb; that is, rate of climb divided by velocity along flight path

Charts showing values of $(D/L)_o$ can be calculated
by the method outlined in reference 1 for any desired
value of P/L by inclusion of the shaft-torque coeffi-
cient

$$\frac{2C_Q}{\sigma} = \frac{P}{L} a \left(\mu \frac{2C_T}{\sigma a} \right)$$

where

C_Q torque coefficient

σ solidity; ratio of total blade area to swept-
            disk area

a slope of lift coefficient against section angle
            of attack (radian measure)

μ tip-speed ratio

C_T thrust coefficient

in the equation expressing the torque equilibrium of the
rotor. (See section entitled "Application of Theory" in
reference 1.) The expression for $\mu \frac{2C_T}{\sigma a}$ is given in
equation (14) of reference 1.

Rotor characteristics.- The sample rotor for which
the charts presented herein were prepared was assumed to
have hinged rectangular untwisted blades. A value of
the mass factor γ of 15 was used. The charts are con-
sidered applicable to rotors having values of γ ranging
from 0 to 25.

Airfoil characteristics.- The airfoil characteristics
assumed in reference 1 were used in preparing the charts.
The equation representing the section profile-drag coef-
ficient is

$$c_{d_o} = 0.0087 - 0.0216\alpha_o + 0.400\alpha_o{}^2$$

where α_o is the section angle of attack. The corre-
sponding profile-drag curve is shown in figure 1 with
experimental curves for several typical airfoils.

Limits of validity of theory.- As was explained in
reference 1, calculations based on the representation of
the airfoil drag characteristics by a power series of
three terms become optimistic when high blade angles are
encountered over too large a portion of the rotor disk.
It should be noted, however, that very little improvement
in $(D/L)_O$ is to be expected by operating beyond the
conditions to which the theory is limited, as a result
of the rapidity of growth of the region of high angle
of attack. This fact is readily demonstrated by
graphical treatments for both autogiro and helicopter
cases.

In the example given for the autogiro in refer-
ence 1, a satisfactory limit was found to be the con-
dition in which a blade element at an azimuth angle of
270° and having a relative velocity $u_T\Omega R$ equal to four-
tenths the rotational tip speed reached an angle of
attack of 11.75^O. The use of this locus line has been
retained in the present example but, for convenience,
the angle of attack has been increased to an even 12°.
Because the limiting angle of attack depends upon the
section and upon the Reynolds number and Mach number,
an additional locus line has been included for an angle
of attack of 16°. For values of P/L greater than
about 0.1, the highest blade angles are encountered at
the blade tip instead of inboard; hence, locus lines
for angles of attack of 12° and 16° at the blade tip, at
an azimuth angle of 270°, are substituted for those for
$u_T = 0.4$ whenever the tip locus lines fall above those
for $u_T = 0.4$.

In the charts presented herein, the locus lines for
the conditions for which a blade element at an azimuth
angle of 270° with a relative velocity $u_T\Omega R$ equal to
four-tenths the rotational tip speed reached a specified
angle of attack are designated by the symbol
$\alpha_{(u_T=.4)(270^O)}$. Similarly, the locus lines for the
conditions for which the blade tip at an azimuth angle
of 270° reached a specified angle of attack are desig-
nated by the symbol $\alpha_{(1.0)(270^O)}$.

RESULTS

The charts of $(D/L)_O$ obtained for the sample
rotor are shown in figure 2. The chart for $P/L = 0$,

that is, for autorotation, is the same as figure 3 of reference 1 except for the choice of limit lines. A value of P/L of 0.2 may be considered as typical of present helicopters at or near cruising speed. Values lower than 0.2 correspond to cleaner craft or to a power-on glide. Higher values correspond to less stream-lined craft or to a positive angle of climb; the highest value covered by the present charts, P/L = 0.5, may be viewed as representing a typical helicopter climbing at an angle of approximately 15° or 20°.

DISCUSSION

Inspection of the charts reveals that the effect of increasing power on the optimum $(D/L)_o$, as indicated by the lowest points on the limit lines, is to produce a moderate but progressive increase in the magnitude of the value of $(D/L)_o$ and to shift the optimum tip-speed ratio toward lower values. It may be remarked that similar charts for twisted blades show a relatively insignificant increase in $(D/L)_o$, up to values of P/L of 0.2 or higher.

As has already been noted, for both helicopter and autogiro conditions, the optimum $(D/L)_o$ is indicated as being obtained at the highest pitch angles permitted by the section angles of attack encountered on the retreating side of the rotor disk. The choice of pitch angles materially lower than those corresponding to the locus lines for an angle of attack of 12° results in extreme inefficiency.

SAMPLE PERFORMANCE CALCULATION

Power absorbed by main rotor.- In order to illustrate the manner in which the charts may be used to estimate the power required by a helicopter under a given set of conditions, an example has been included.

Assume a helicopter to be operating in level flight at sea level under the following conditions:

Forward speed, feet per second........................ 80   *400 fps*
Tip-speed ratio, μ 0.2
Disk loading, pounds per square foot 2.5

Disc Area = 1256 Sq FT

handwritten: BLADE AREA = 20 × 2 × .22 = 88 SQ FT

handwritten: = 3140 / .001189 × 1256 × 80²

6

handwritten: chord .22'

Gross weight, pounds 3140
Rotor radius, feet 20
Blade plan form .... Rectangular
Blade twist .... None
σ Solidity 0.07
Parasite-drag area, square feet 15

For these assumptions, $C_L = 0.329$ and $\dfrac{C_L}{\sigma} = 4.70$.
In order to obtain a first approximation to $(D/L)_0$ for
use in equation (1), P/L is assumed to be 0.2. Fig-
ure 2(e) then gives a value of 0.086 for $(D/L)_0$ at the
intersection of the curve for $\mu = 0.2$ with the line for
$\dfrac{C_L}{\sigma} = 4.70$. The value of $(D/L)_i$, as indicated in refer-
ence 1, is simply $C_L/4$ or 0.082. The parasite drag-
lift ratio is

$$\left(\frac{D}{L}\right)_p = \frac{0.001189 \times 15 \times (80)^2}{3140}$$
$$= 0.036$$

Since the rate of climb is assumed zero, the value
of P/L from equation (1) is

$$\frac{P}{L} = 0.086 + 0.082 + 0.036 + 0$$
$$= 0.204$$

As a second approximation, the value of $(D/L)_0$ may
be obtained by interpolation between the charts for
$\dfrac{P}{L} = 0.20$ and for $\dfrac{P}{L} = 0.25$. The value so obtained is,
within the limits of accuracy in reading the charts, equal
to the original value of 0.086 and no further approxima-
tions are necessary.

The total rotor-shaft power required for the specified
condition may now be calculated as

$$\frac{0.204 \times 3140 \times 80}{550} = 93.2 \text{ horsepower}$$

Power absorbed by auxiliary rotor.- The charts may
also be used to estimate the power absorbed by the tail
rotor.

Assume that the torque of the main rotor is being
counteracted by an articulated auxiliary rotor having
the following characteristics:

Blade plan form .... Rectangular
Blade twist .... None
Solidity 0.10

Spindle angle, α, degrees 0
Distance between spindle and main
    rotor axis, feet 25
Radius, feet 4
Tip-speed ratio 0.2

The tail-rotor thrust, based on the main-rotor power already calculated, is 102.7 pounds and the corresponding thrust coefficient C_T is 0.00536. The inflow-velocity factor λ may be obtained from equation (8) of reference 1

$$\alpha = \frac{\lambda}{\mu} + \frac{C_T}{2\mu^2}$$

Substitution of the values for the present case gives a value of $\lambda = -0.0134$. By using a lift-curve slope a of 5.73 per radian, substitution of this value of λ in equation (6) of reference 1 gives a blade pitch angle θ of 4.47°.

In order to permit the use of the charts of figure 2, it is convenient to calculate the value of C_L/σ from the relation

$$\frac{C_L}{\sigma} = \frac{2C_T}{\bar{\sigma}\mu^2}$$

which gives a value of $\frac{C_L}{\sigma} = 2.68$. The value of P/L corresponding to the specified combination of values μ, θ, and C_L/σ is found by interpolation between figures 2(c) and 2(d) to be 0.138.

The auxiliary-rotor shaft power is then

$$\frac{0.138 \times 102.7 \times 80}{550} = 2.1 \text{ horsepower}$$

Since the auxiliary rotor may also be producing a drag, the total power charged to torque counteraction should be calculated from the sum of the values of $(D/L)_0$ and $(D/L)_i$. The value of $(D/L)_0$ at $P/L = 0.138$, by interpolation from figure 2, is 0.120. The value of $(D/L)_i$ is

$$\left(\frac{D}{L}\right)_i = \frac{c_L}{\sigma}\frac{\sigma}{4}$$
$$= 0.268\,\frac{0.1}{4}$$
$$= 0.067$$

The total drag-lift ratio is then 0.187 and the corresponding power is 2.8 horsepower. The difference between the two values of power results from the drag on the auxiliary rotor and hence must be supplied through the main-rotor shaft; the revised value of main-rotor shaft power is then 93.9 horsepower.

If a particularly rigorous treatment is desired, the difference between the auxiliary-rotor values of $(D/L)_o + (D/L)_i$ and P/L should be converted into a drag-lift ratio based on the main-rotor lift, that is, $0.049\,\frac{102.7}{3140}$ or 0.002 for the present case. This value should then be added to the original value of $(D/L)_p$ used in the main-rotor calculations, and the entire procedure repeated. Examination of the problem has shown, however, that the differences so obtained are negligible for normal ranges of variables, since the rotor profile drag-lift ratio is not particularly sensitive to the value of P/L used.

CONCLUSIONS

1. The profile drag-lift ratio of a power-driven rotor in forward flight can be completely specified for various combinations of pitch angle, tip-speed ratio, and solidity by a series of charts for different values of power input. On the charts, the profile drag-lift ratio is plotted against the ratio of lift coefficient to solidity for specified values of pitch angle and tip-speed ratio.

2. For a rotor with rectangular untwisted blades, the theoretically derived charts indicate that one effect of increasing the shaft power input is to produce a moderate increase in the profile drag-lift ratio.
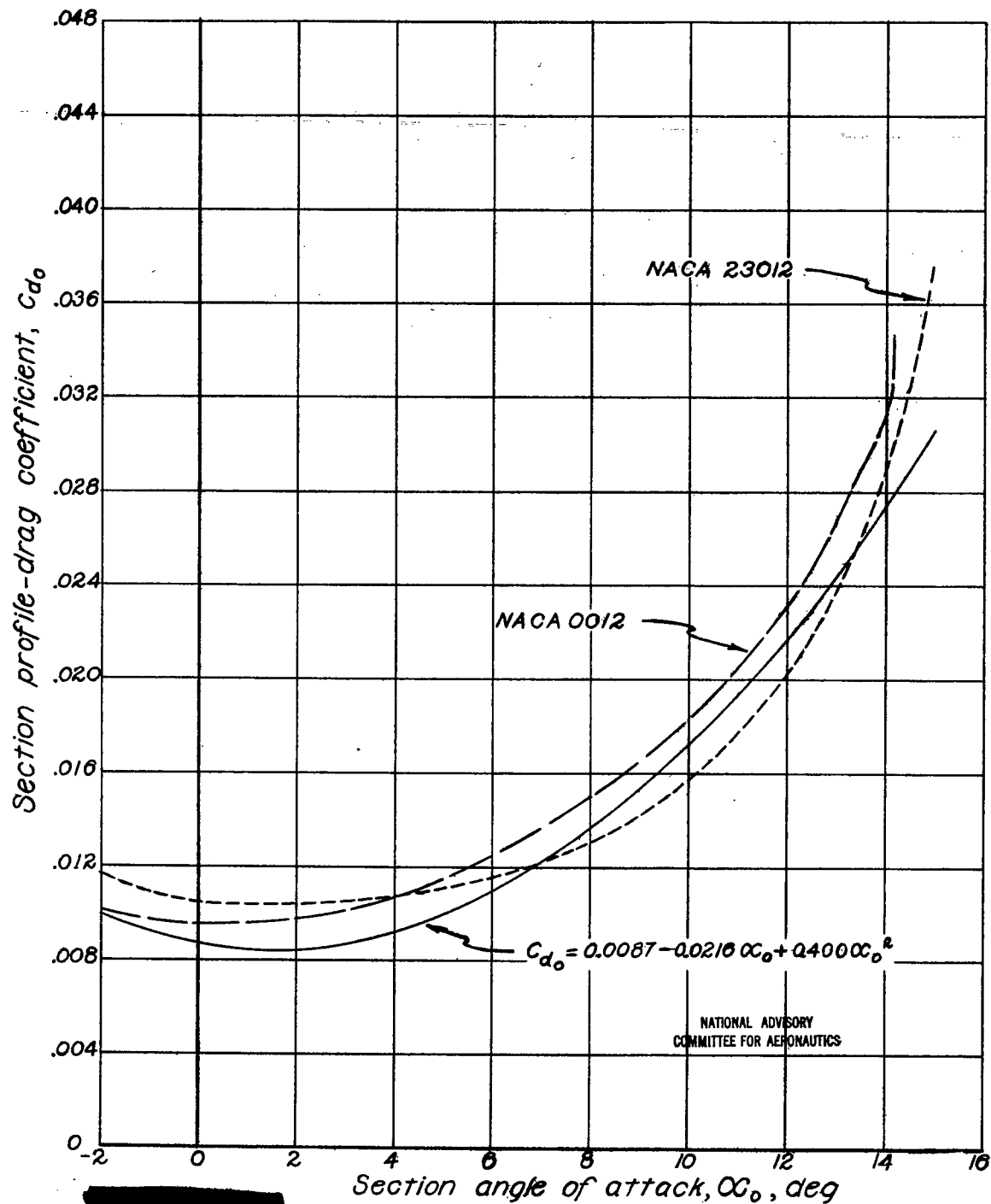
3. Regardless of the amount of power used, the optimum profile drag-lift ratio is obtained at the

highest pitch angles permitted by the high section angles of attack encountered on the retreating side of the rotor disk.

Langley Memorial Aeronautical Laboratory
    National Advisory Committee for Aeronautics
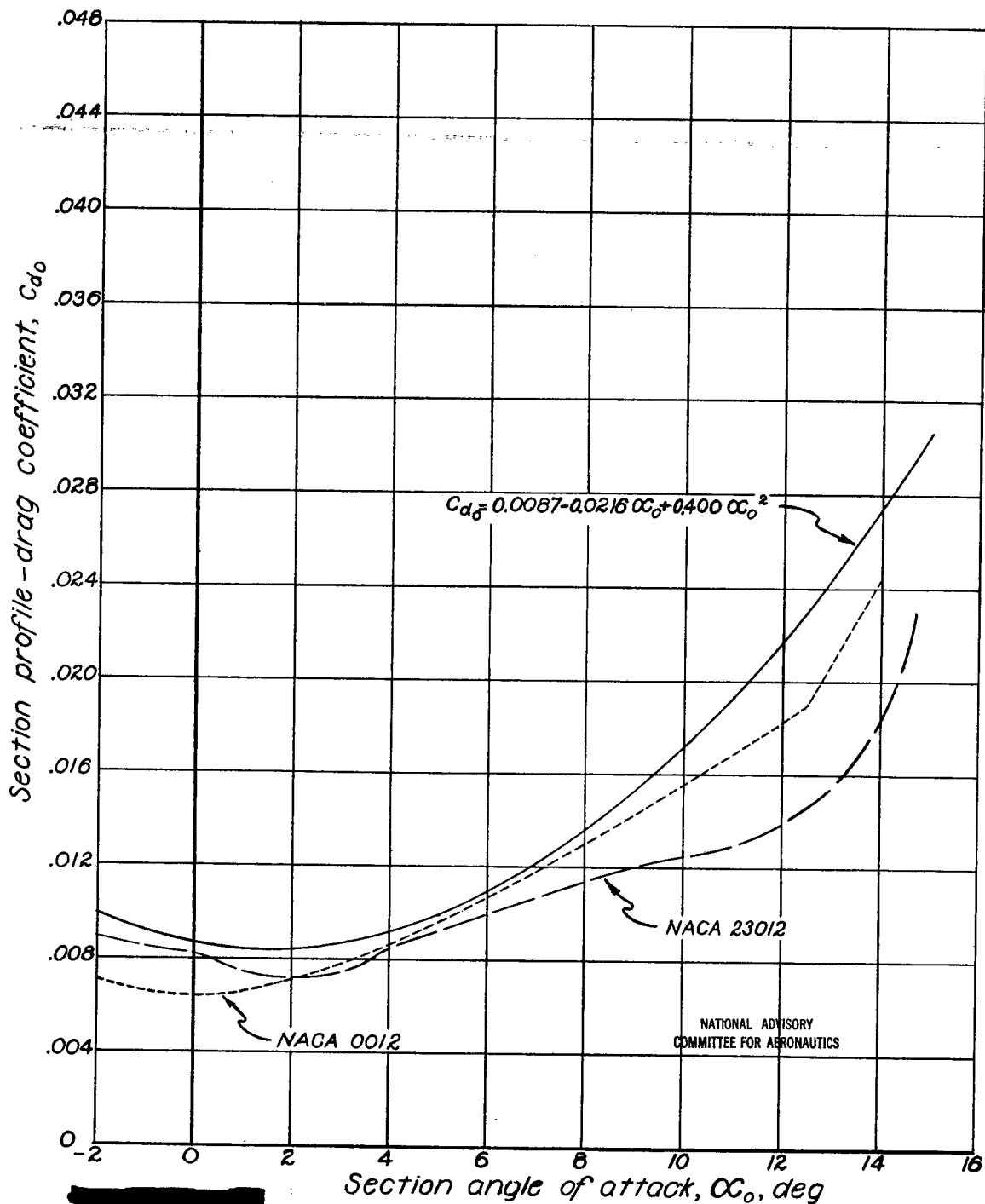   Langley Field, Va.

REFERENCES

1. Bailey, F. J., Jr.: A Simplified Theoretical Method of Determining the Characteristics of a Lifting Rotor in Forward Flight. NACA Rep. No. 716, 1941.

2. Jacobs, Eastman N., and Sherman, Albert: Airfoil Section Characteristics as Affected by Variations of the Reynolds Number. NACA Rep. No. 586, 1937.

3. Jacobs, Eastman N., and Clay, William C.: Characteristics of the N.A.C.A. 23012 Airfoil from Tests in the Full-Scale and Variable-Density Tunnels. NACA Rep. No. 530, 1935.

4. Goett, Harry J., and Bullivant, W. Kenneth: Tests of N.A.C.A. 0009, 0012, and 0018 Airfoils in the Full-Scale Tunnel. NACA Rep. No. 647, 1938.

5. Tetervin, Neal: Tests in the NACA Two-Dimensional Low-Turbulence Tunnel of Airfoil Sections Designed to Have Small Pitching Moments and High Lift-Drag Ratios. NACA CB No. 3I13, 1943.

$$C_{d_0} = 0.0087 - 0.0216\,\alpha_0 + 0.400\,\alpha_0^2$$

NACA 23012

NACA 0012

NATIONAL ADVISORY
COMMITTEE FOR AERONAUTICS

(a) Data from NACA variable-density tunnel; Reynolds number, 2.6 x 10⁶; reference 2.

Figure 1.- Comparison of the power-series profile-drag curve used in the analysis with experimental data on representative airfoil sections.
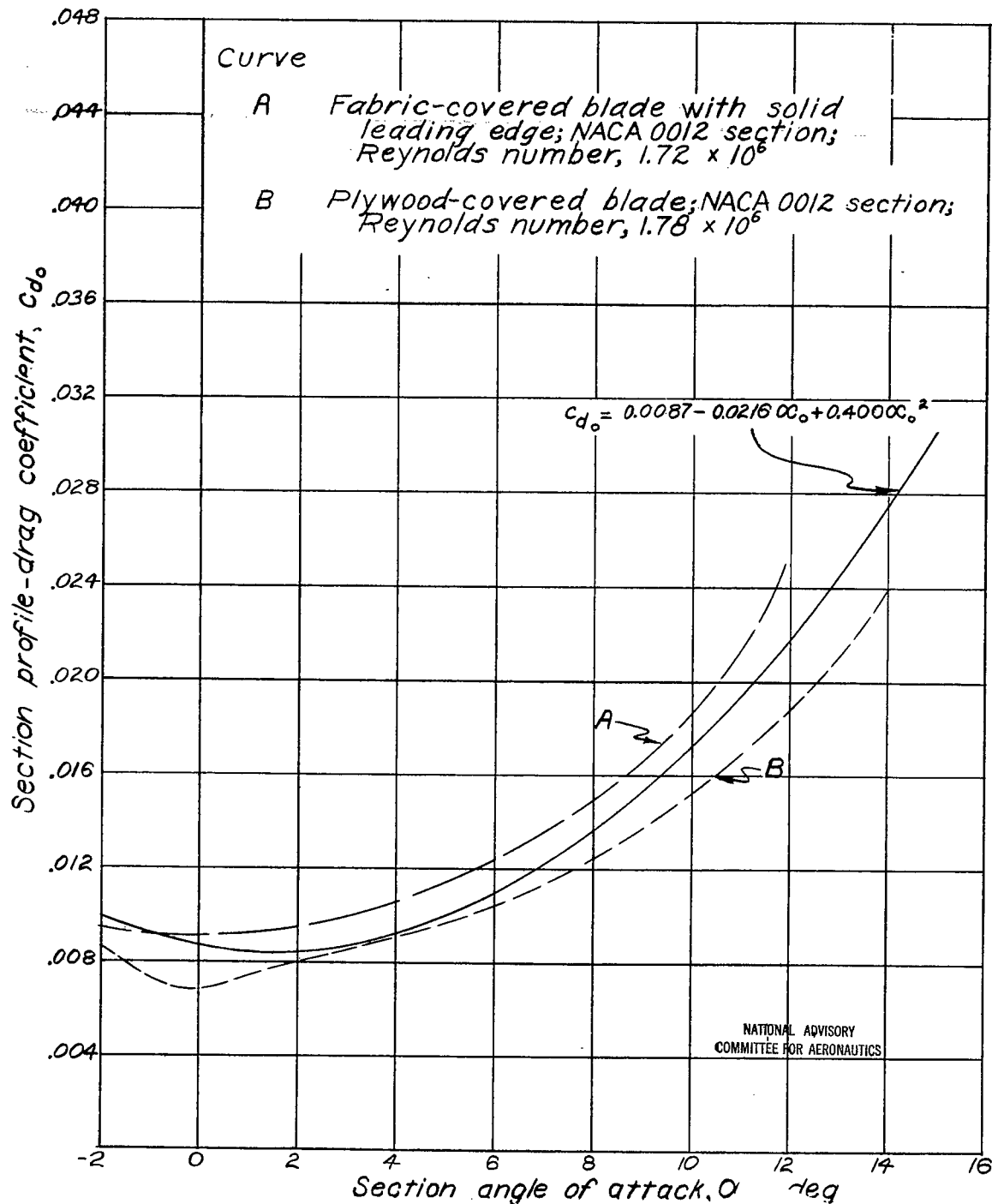
$$C_{d_o} = 0.0067 - 0.0216\,\alpha_o + 0.400\,\alpha_o{}^2$$

NACA 23012

NACA 0012

NATIONAL ADVISORY
COMMITTEE FOR AERONAUTICS

Section angle of attack, α_o, deg

Section profile-drag coefficient, C_{d_o}

(b) Data from NACA full-scale tunnel; Reynolds number, 3.4×10^6; references 3 and 4.

Figure 1.- Continued.
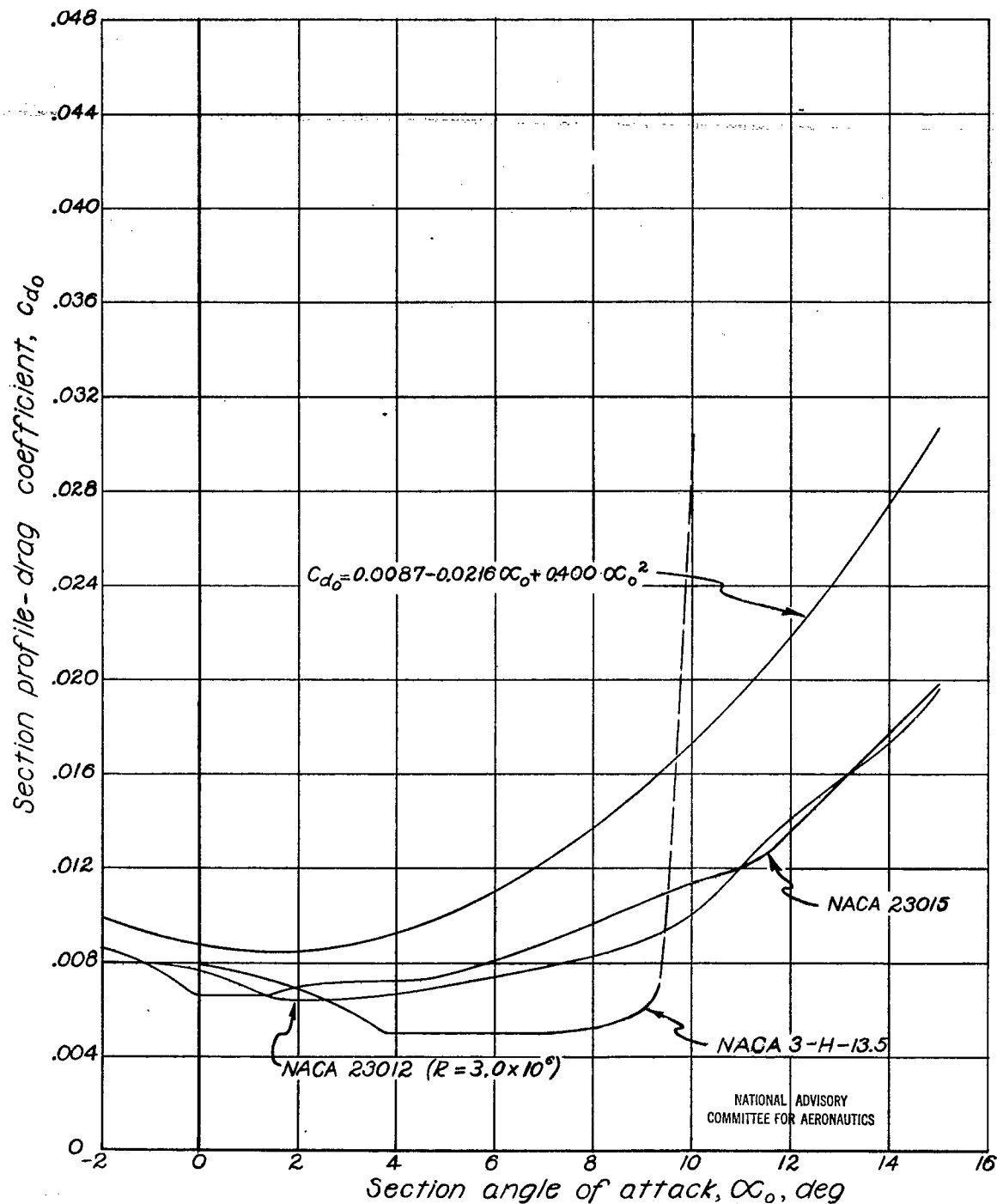
(c) Data from NACA two-dimensional low-turbulence tunnel and
   NACA two-dimensional low-turbulence pressure tunnel;
   Reynolds number, 2.6 x 10^{6}; reference 5 and unpublished
   data.

Figure 1.- Continued.

Curve

A   Fabric-covered blade with solid
leading edge; NACA 0012 section;
Reynolds number, 1.72×10^6

B   Plywood-covered blade; NACA 0012 section;
Reynolds number, 1.78×10^6

$$c_{d_o} = 0.0087 - 0.0216\,\alpha_o + 0.4000\,\alpha_o{}^2$$

A

B

Section profile-drag coefficient, c_{d_o}

Section angle of attack, α deg

(d) Data on practical-construction rotor-blade specimens, from
NACA two-dimensional low-turbulence pressure tunnel;
unpublished data.

Figure 1.- Concluded.
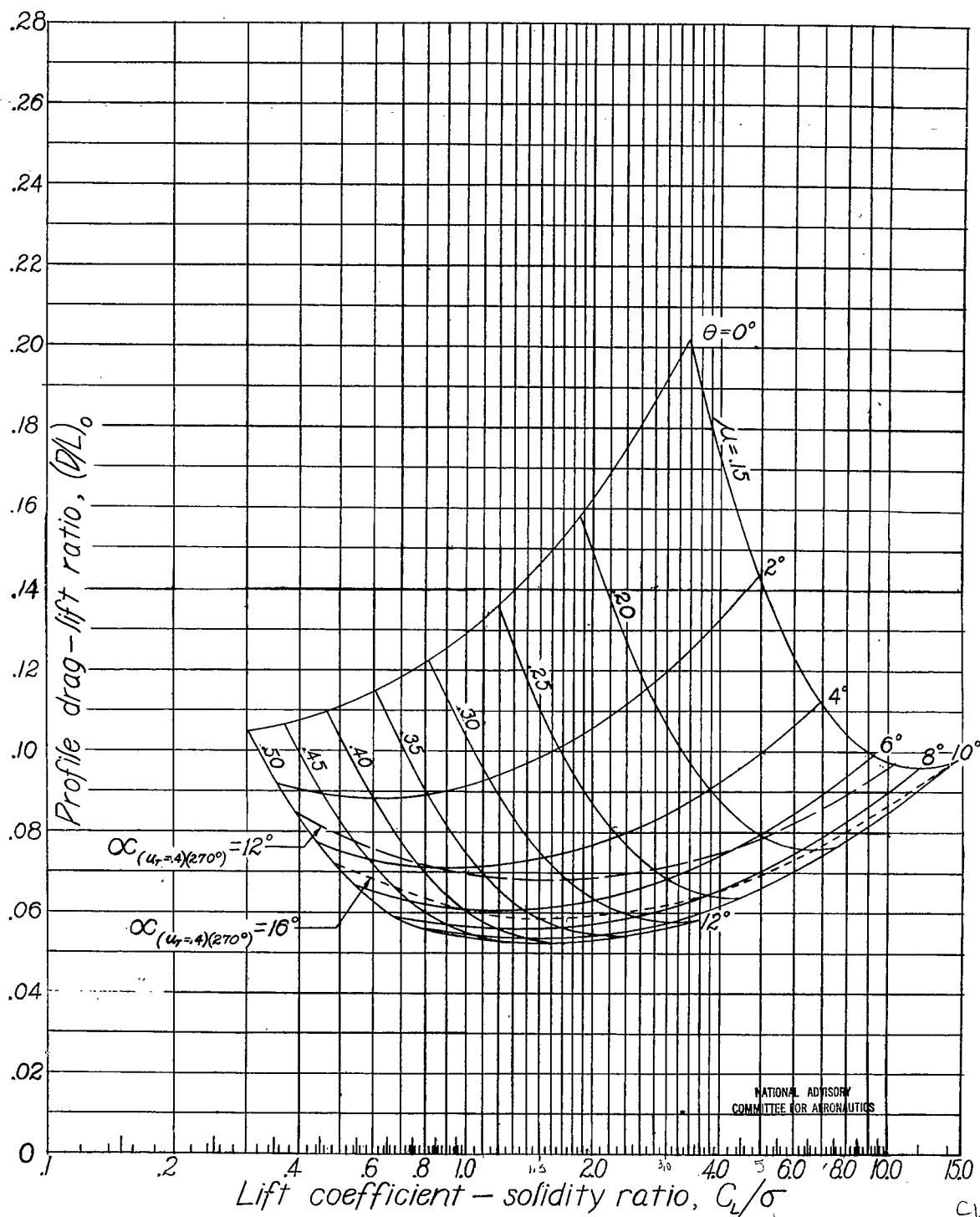
(a) $P/L = 0$.

Figure 2.— Profile drag-lift ratio for sample rotor.
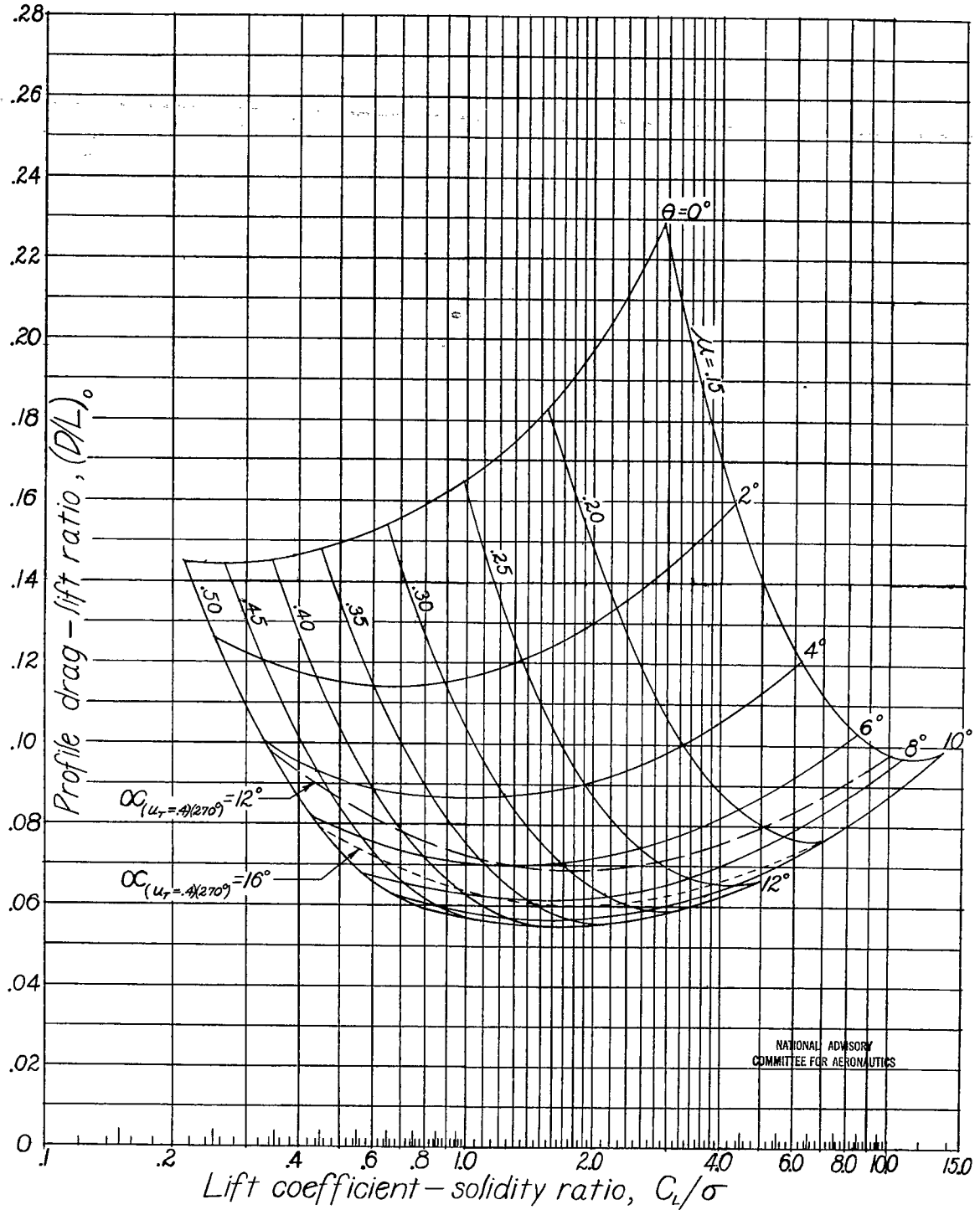
(b) $P/L = .05$.

Figure 2.— Continued.
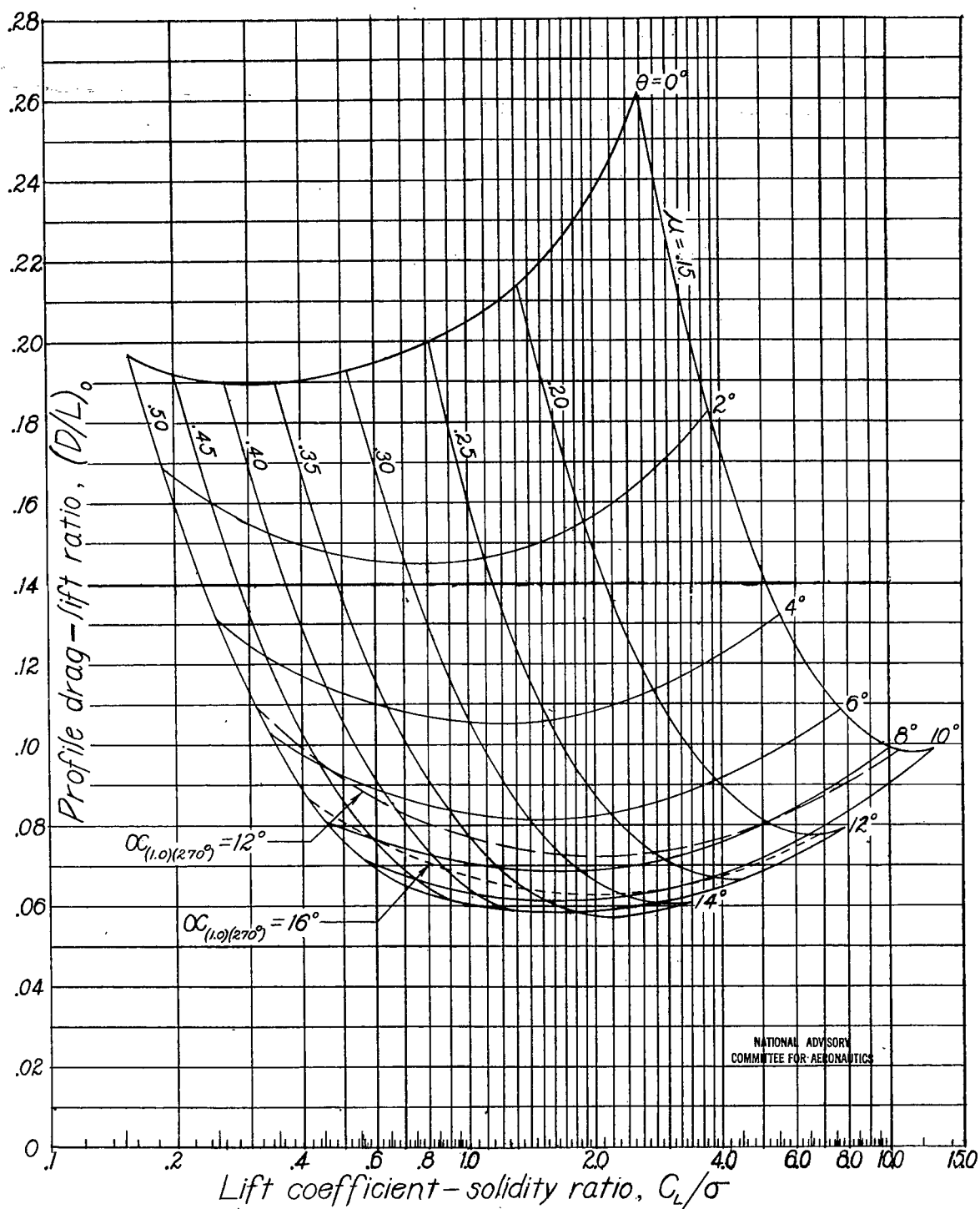
(c) P/L = .10.

Figure 2.– Continued.
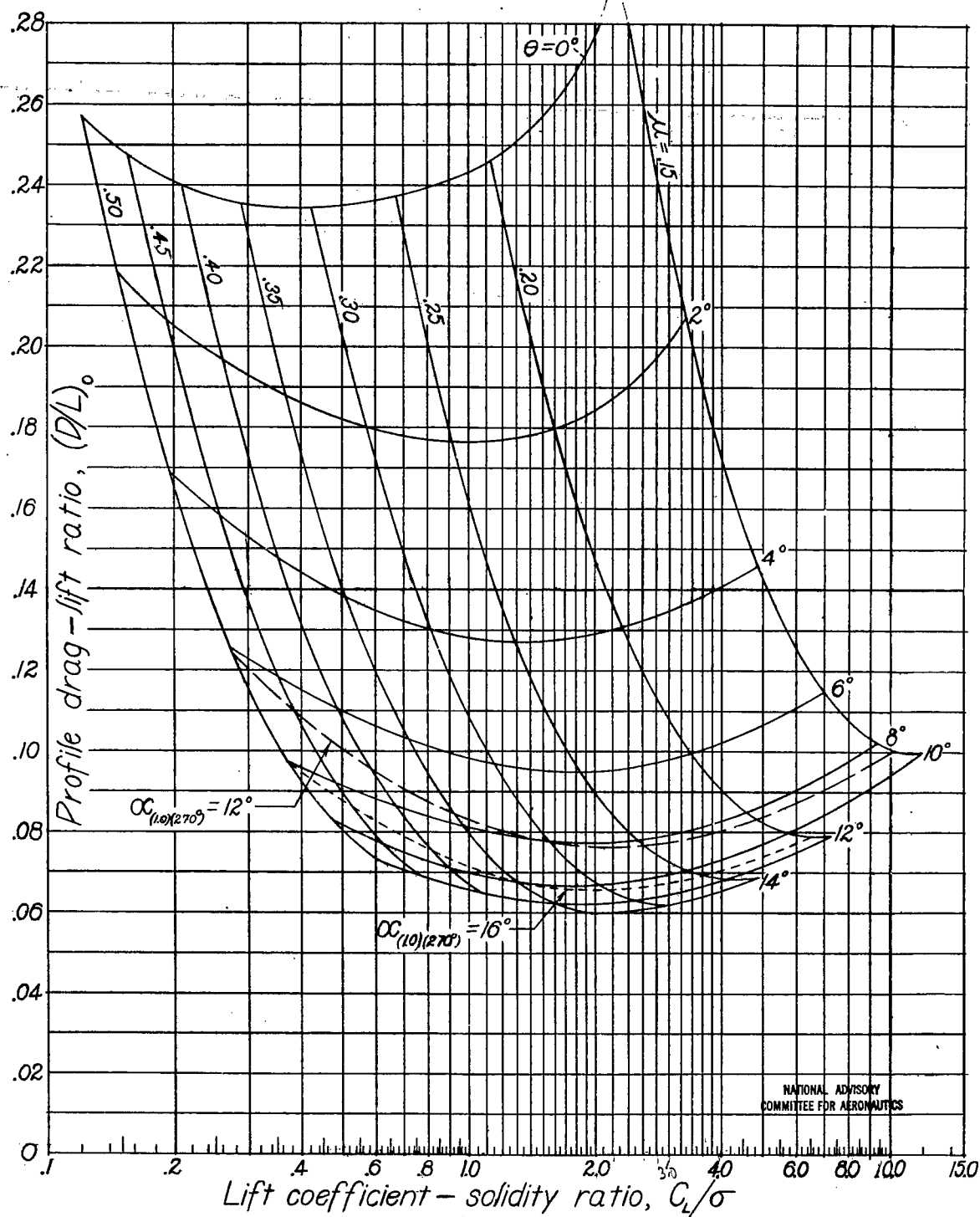
(d) $P/L = .15$.

Figure 2.— Continued.
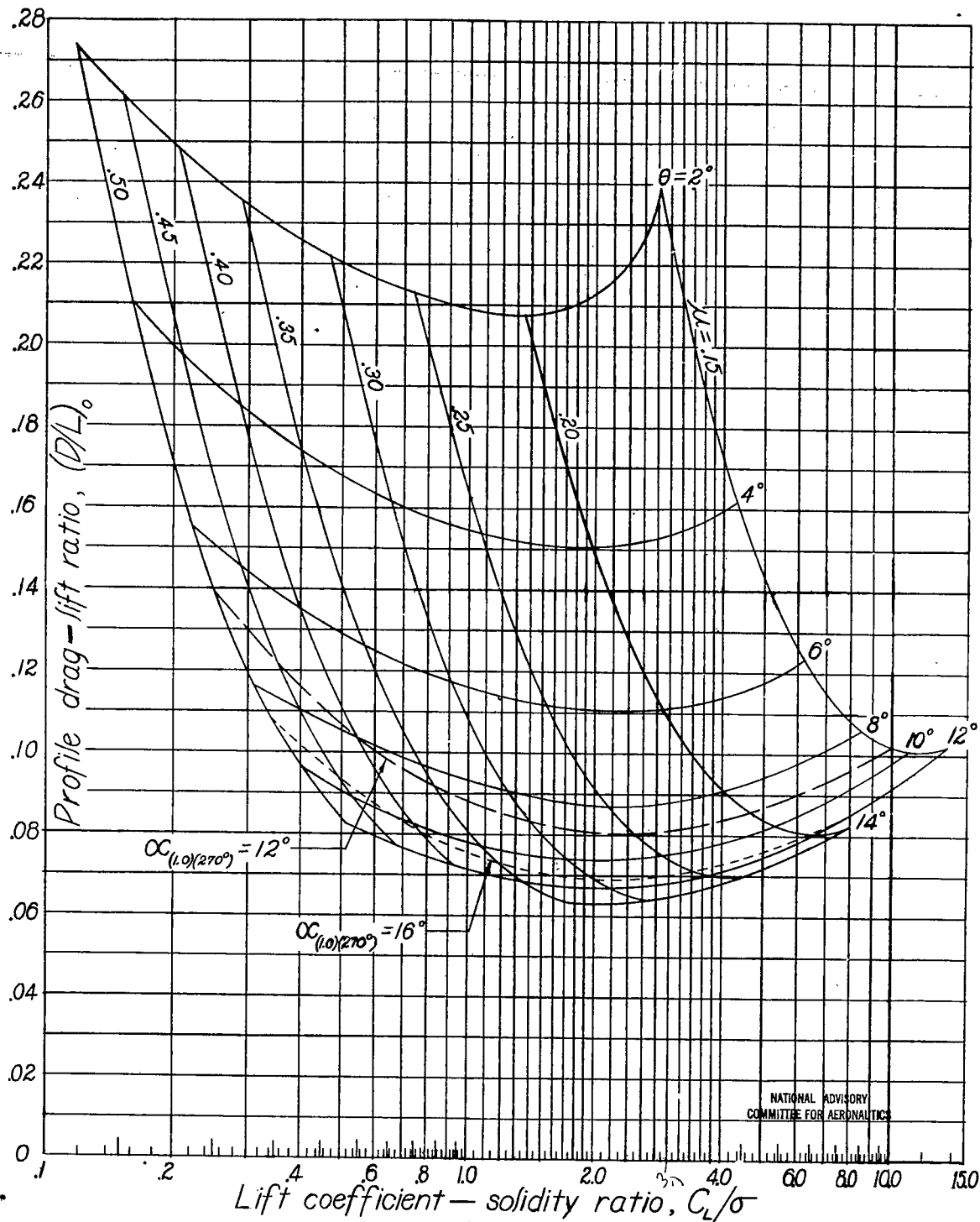
(e) P/L = .20.

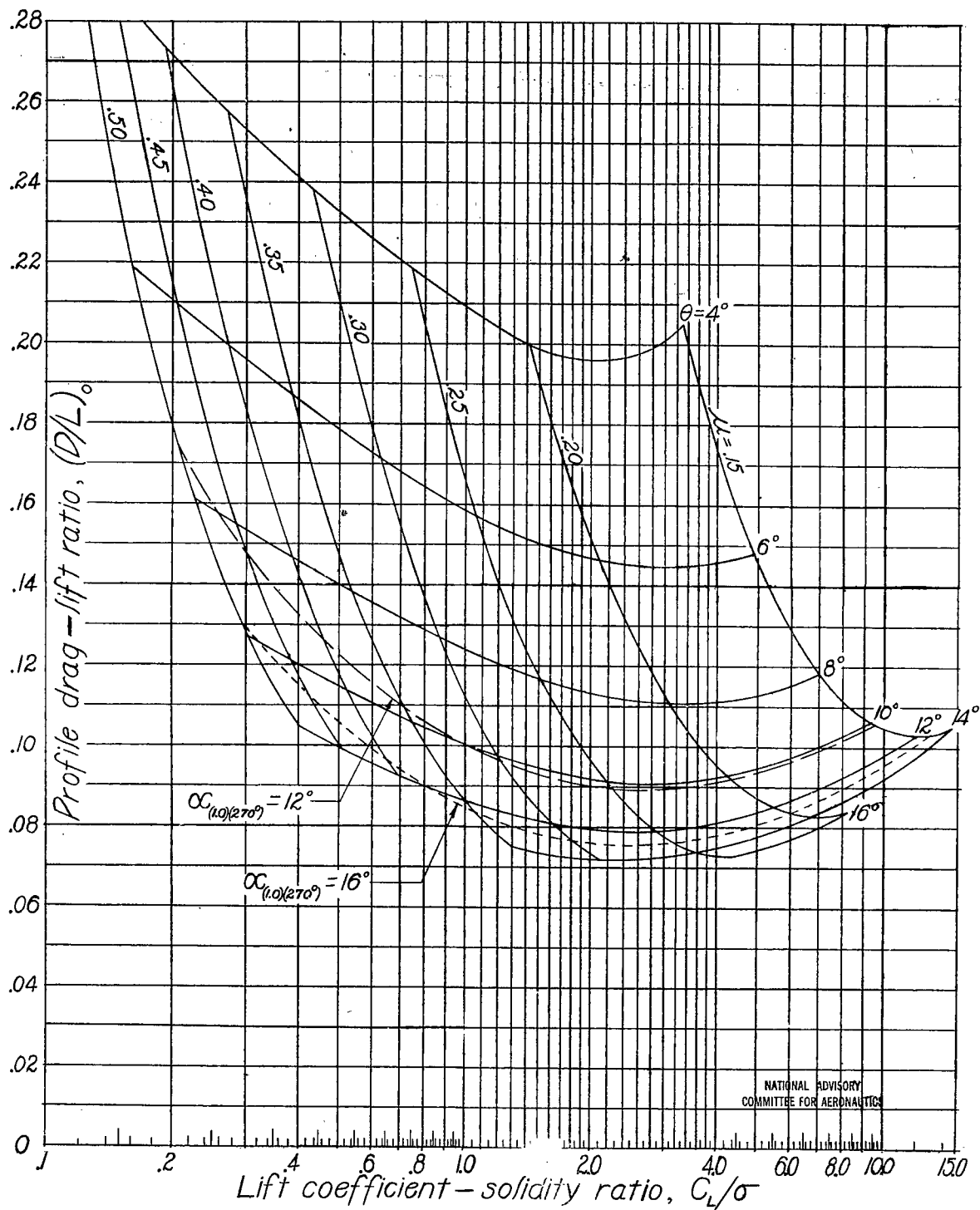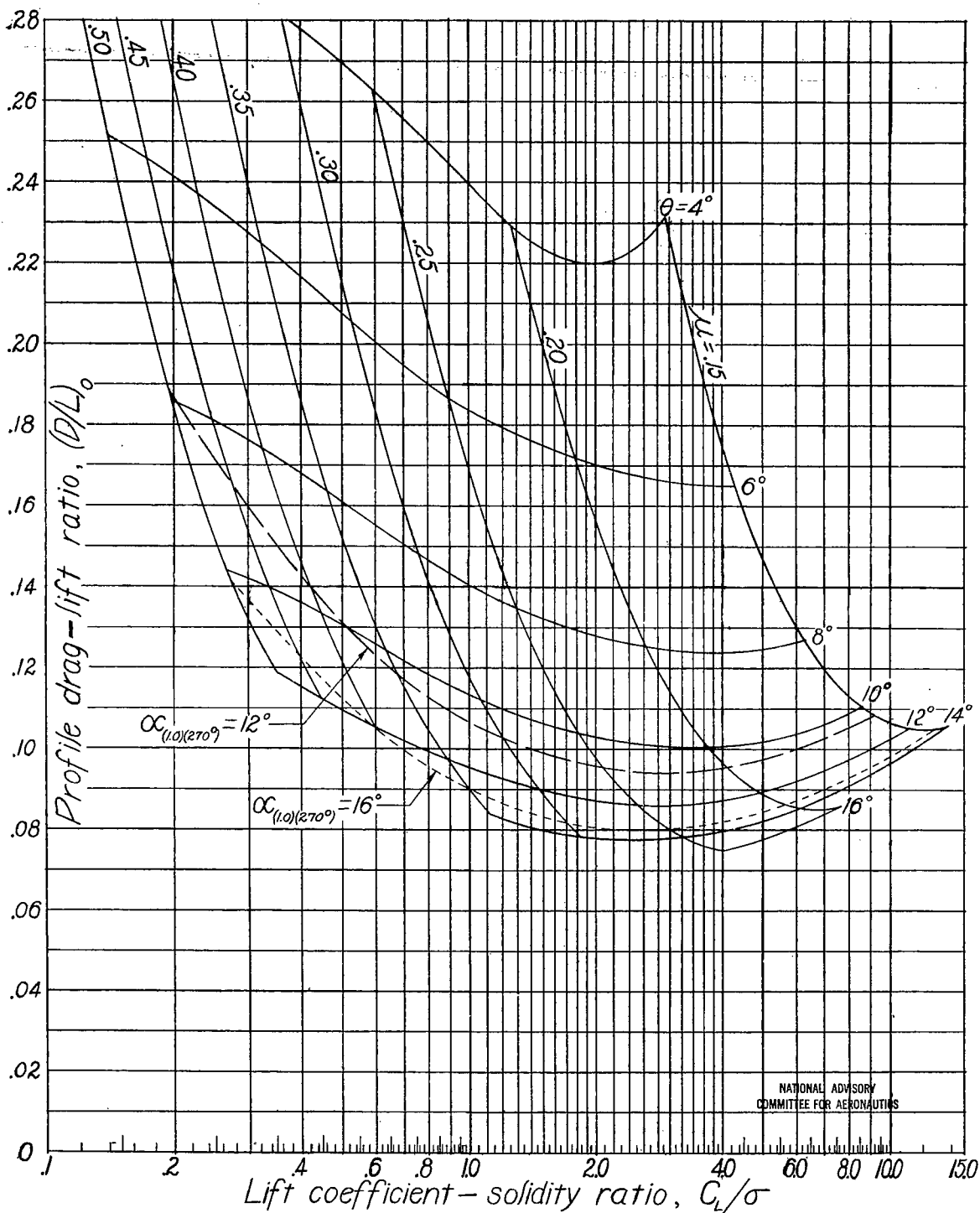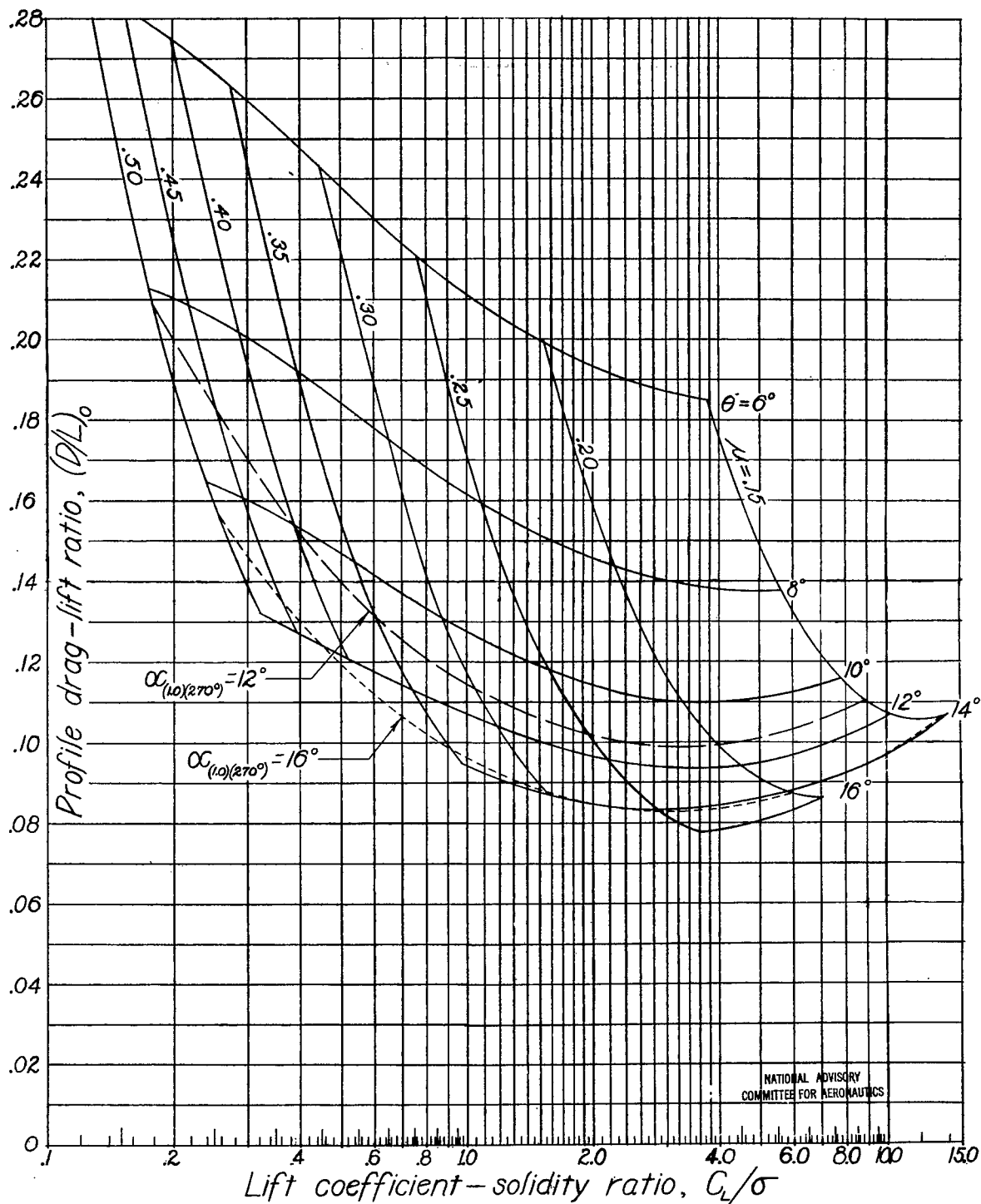Figure 2.— Continued.
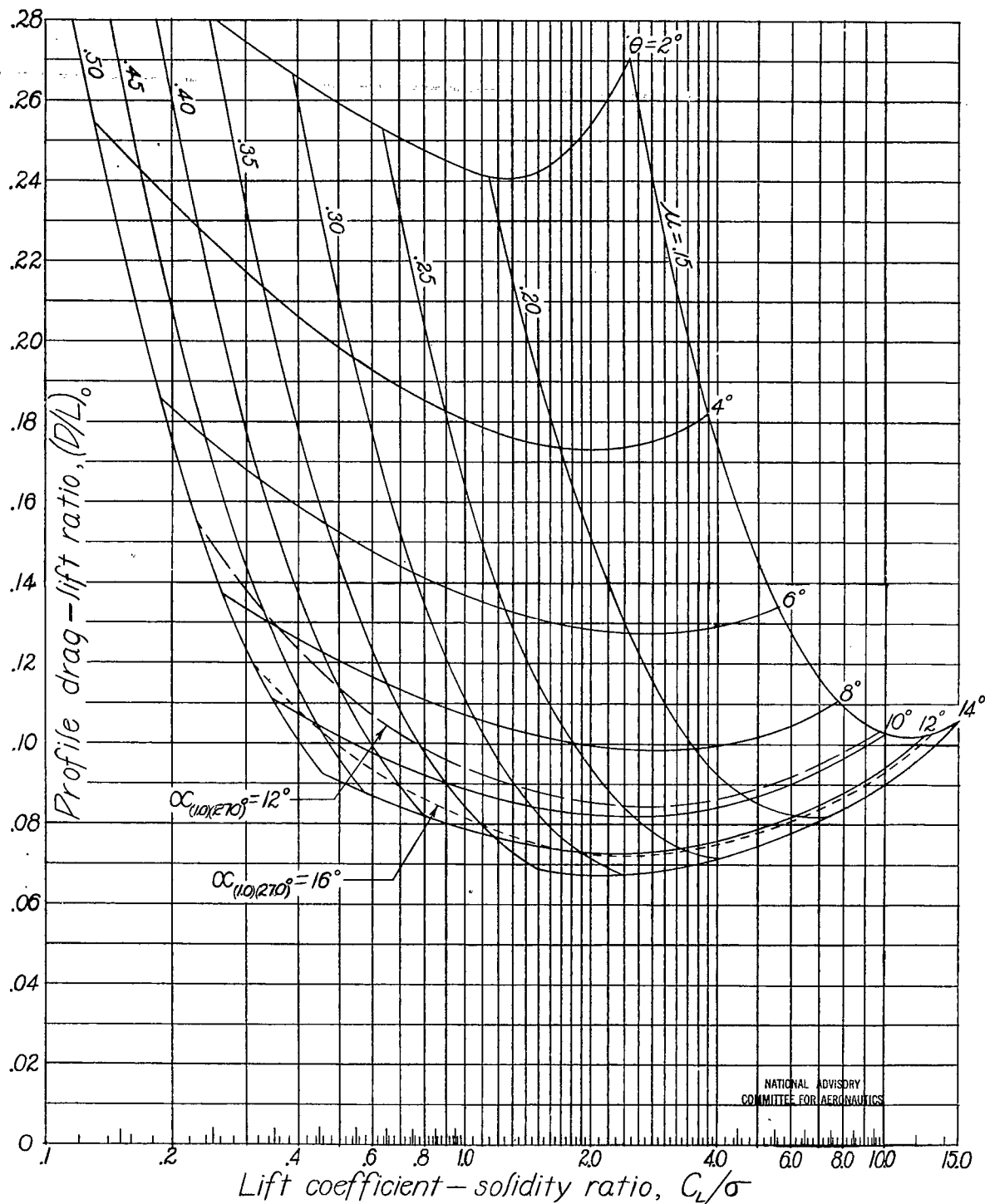
(f) P/L = .25.

Figure 2.— Continued.

(g) $P/L = .3($

Figure 2.- Continued.

(h) P/L = .35.

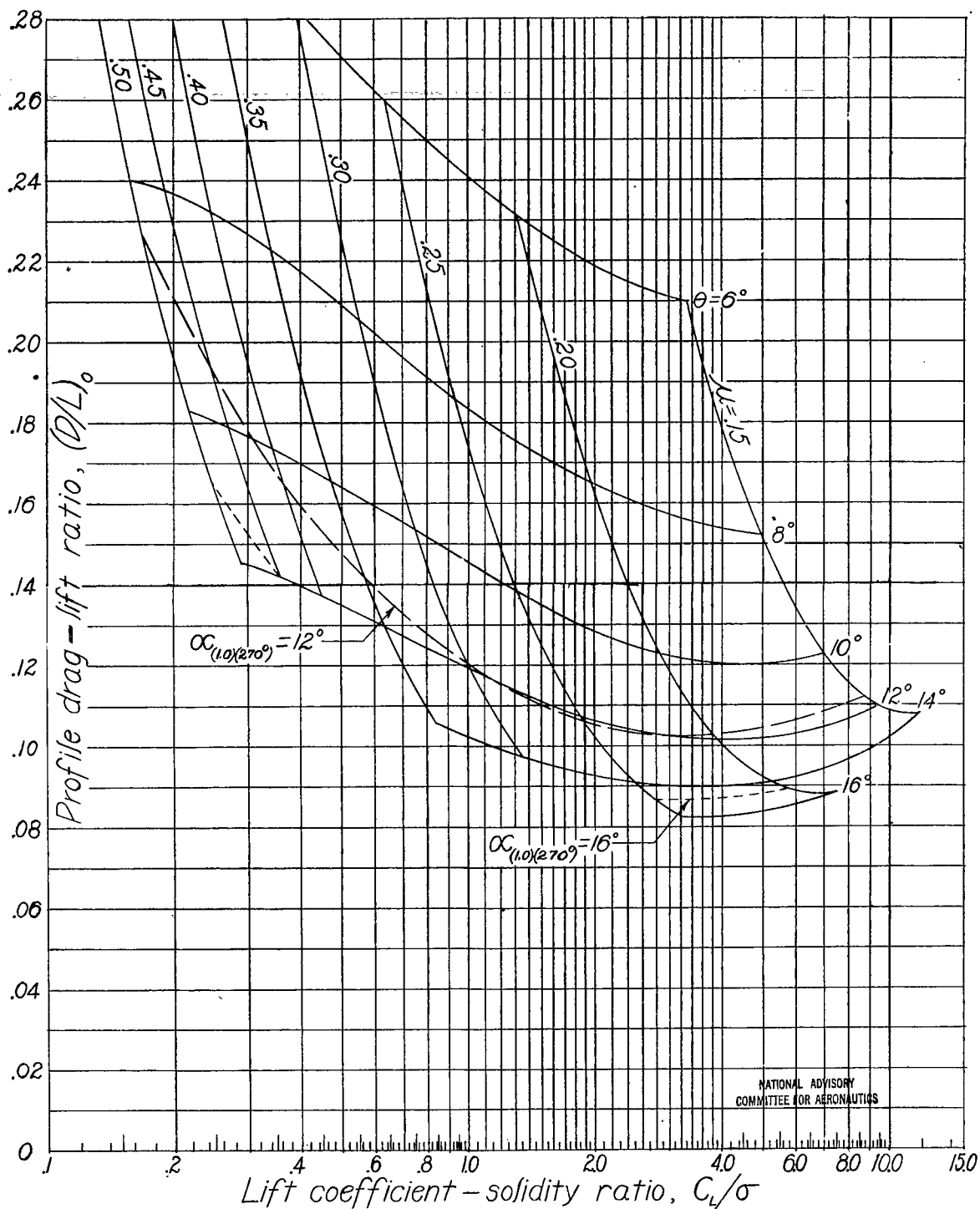Figure 2.– Continued.
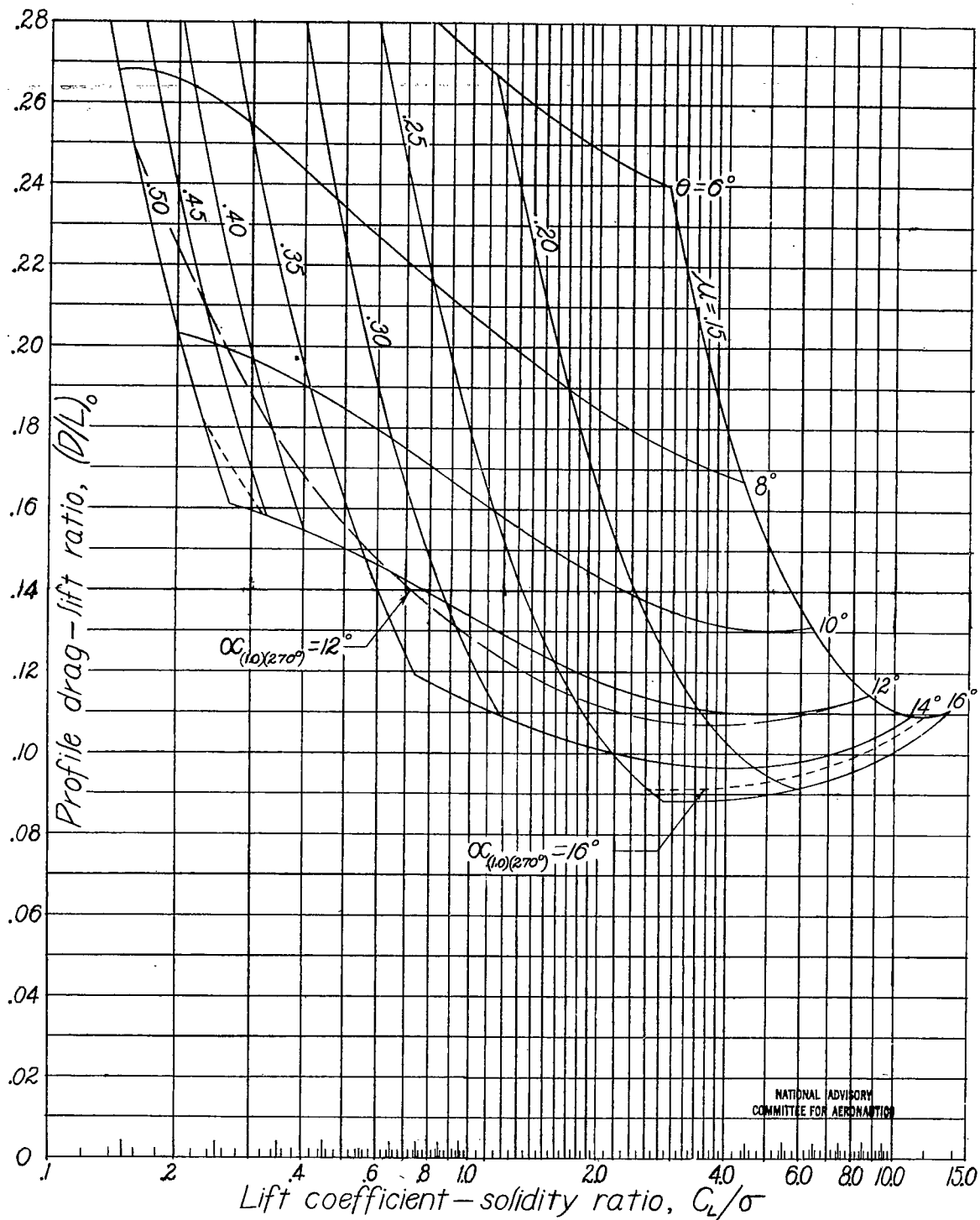
(i) P/L=.40.

Figure 2.— Continued.

(j) P/L = .45.

Figure 2.– Continued.

(k) P/L = .50.

Figure 2.— Concluded.